All Optical Full Adder Based on Intramolecular Electronic Energy Transfer in the Rhodamine–Azulene Bichromophoric System

ARTICLE *in* THE JOURNAL OF PHYSICAL CHEMISTRY C · SEPTEMBER 2008

Impact Factor: 4.77 · DOI: 10.1021/jp804658b

6 AUTHORS, INCLUDING:

Yoav Eichen
Technion - Israel Institute of Technology
108 PUBLICATIONS **3,507** CITATIONS
SEE PROFILE

F. Remacle
University of Liège
185 PUBLICATIONS **3,524** CITATIONS
SEE PROFILE

Raphael D. Levine
Hebrew University of Jerusalem
200 PUBLICATIONS **4,899** CITATIONS
SEE PROFILE

Shammai Speiser
Technion - Israel Institute of Technology
307 PUBLICATIONS **2,012** CITATIONS
SEE PROFILE

All Optical Full Adder Based on Intramolecular Electronic Energy Transfer in the Rhodamine−Azulene Bichromophoric System

Olga Kuznetz,[‡] Husein Salman,[‡] Yoav Eichen,[‡] F. Remacle,[§,†] R. D. Levine,[⊥] and Shammai Speiser*[,‡]

Schulich Faculty of Chemistry, Technion - Israel Institute of Technology, Haifa 32000, Israel, Department of Chemistry, B6c, University of Liege, B4000 Liege, Belgium, and Fritz Haber Research Center, Hebrew University, Jerusalem 91904, Israel

Received: May 27, 2008; Revised Manuscript Received: July 21, 2008

Charge and electronic energy transfer (ET and EET) are well-studied examples whereby different molecules can signal their state from one (the donor, D) to the other (the acceptor, A). The electronic energy transfer from the donor (Rh) to the acceptor (Az) is used to build an all-optical full adder on a newly synthesized bichromophoric molecule Rh−Az. The results are supported and interpreted by a full kinetic simulation. It is found that the optimal design for the implementation of the full adder relies in an essential way on the intramolecular transfer of information from the donor to the acceptor moiety. However, it is not the case that the donor and the acceptor each act as a half adder.

Introduction

A full adder adds two binary numbers and also takes into consideration a carry from a previous addition. There are three inputs. Since each input is binary, there are eight distinct input triplets. These generate four output doublets consisting of the values of the two outputs, the sum, and the new carry digit. (The explicit input−output correspondence is shown in a truth table shown below; Table 1.) In an all-optical case, the 3 inputs, at the frequency ω_i, as well as the sum out and carry out outputs are optical signals. Several implementations of logic circuits, including full adders, have already been reported at the molecular level.[1−7] In conventional computer circuits, a full adder is typically realized by the concatenation of two half adders.[1] While a donor−acceptor could be a candidate for such an implementation of a full adder, we show in this paper, using the support of a kinetic model, that for the particular molecular system under study, a more optimal way is to map directly the photophysics onto a full addition without an intermediate decomposition into two concatenated half adders. The scheme proposed uses in an essential way the transfer of information from the donor to the acceptor molecule. This was the idea in our original work,[2] and it has since been applied also in the implementation of a full adder on the 2-phenylethyl-*N*,*N*-dimethylamine (PENNA) molecule.[3] In both examples, the inputs are provided optically. However, in our previous work,[3] some of the outputs were read by detecting fragments, which means that the molecule self-destructs at the end of the computation. In the scheme discussed here, we can devise a completely optical readout, that is, we are able to realize an all-optical full adder. Moreover, as we demonstrated below, the optical readout can be performed separately for the two outputs of the full adder, the sum out, and the carry out, which are encoded into the laser-induced fluorescence, LIF, yields of two different excited states of the bichromophoric complex.

TABLE 1: Truth Table for a Full Adder

ω_1	ω_2	carry in ≡ ω_3	sum out	carry out
0	0	0	0	0
1	0	0	1	0
0	1	0	1	0
0	0	1	1	0
1	1	0	0	1
0	1	1	0	1
1	0	1	0	1
1	1	1	1	1

The threshold levels for the optical readout rely on the photoquenching (PQ) effect.[4] This effect is manifested in chromophores that possess several optically active excited electronic states, so that it is possible to excite the lowest excited state, S_1, with one photon and higher excited states, S_n, $n > 1$, with more than one photon, typically two. In this case, a decrease of the fluorescence quantum yield of the S_1 state is observed with increasing exciting light intensity. This comes about because as the intensity increases, the transient population in the S_1 excited level decreases due to excitation to higher S_n states. Thus, this absorbed photon does not contribute to the fluorescence yield for S_1, causing the decrease in the S_1 relative fluorescence quantum yield. Kinetic analysis, under steady-state conditions and for optically thin sample, assuming ultrafast radiationless decay of the S_n ($\geq n$) states back to S_1, yields a "Stern−Volmer" type photoquenching relation (for $n = 2$) given by[4,5]

$$\phi_0/\phi = 1 + \tau_{10}\sigma_{12}I_p \qquad (1)$$

In eq 1, ϕ is the intensity-dependent relative fluorescence quantum yield, ϕ_0 is the relative quantum yield in the absence laser pumping, τ_{10} is the fluorescence lifetime in the absence laser pumping, σ_{12} is the absorption cross section for the $S_1 \rightarrow S_2$ transition (cm^2/molecule), and I_p is the laser pump intensity (photon/cm^2·s). Note that to determine the values of the molecular parameters in eq 1, only measurement of the relative

* To whom correspondence should be addressed. Telephone: + 972 4 8293735. Fax: +972 4 8295703. E-mail: speiser@technion.ac.il.
‡ Technion - Israel Institute of Technology.
§ University of Liege.
† Also the Director of Research at FNRS, Belgium.
⊥ Hebrew University.

10.1021/jp804658b CCC: $40.75
Published on Web 09/12/2008

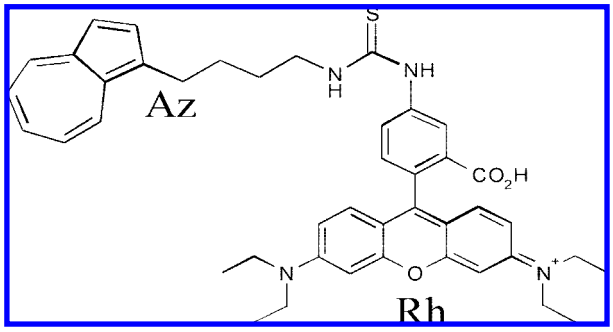

Figure 1. The newly synthesized bichromophoric compound, **Rh**−**Az**.

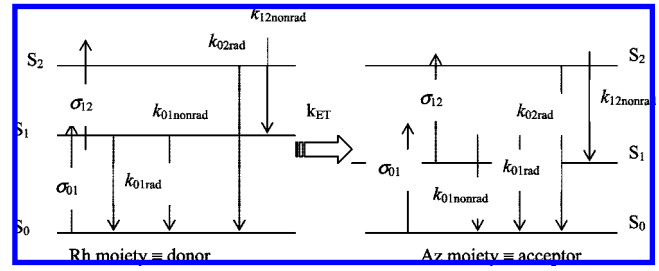

Figure 2. Photophysical processes taken into account in the kinetic scheme used to model the operation of the all-optical molecular full adder.

values of the quantum yields is required. As we discuss in detail in subsection III below, eq 1 allows for arbitrarily setting a threshold for the LIF intensity. Below this threshold, the LIF intensity corresponds to the logical value 0, and above this threshold, it corresponds to a logical value 1.

We have suggested that the Rhodamine (**Rh**)−Azulene (**Az**) molecular system can be used for implementing a molecular full adder, where the communication between the Rh and Az half adder is by $S_1 \rightarrow S_1$ electronic energy transfer (EET).[2] A model **Rh**−**Az** bichromophoric molecule (Figure 1) was synthesized,[6] and its spectral features were examined,[6,7] as well as the $S_1 \rightarrow S_1$ EET process between Rh donor and Az acceptor.[7] A summary of this spectroscopic and EET study is given in subsections II and III below. In addition, preliminary PQ measurements indicate that both moieties function as molecular half adders; however, concatenation by EET does not yield the desired features.[8,9] Yet, these studies have indicated the feasibility of implementing full adder in this molecule by directly employing the photophysics onto a full addition without an intermediate decomposition into two concatenated half adders, which is the subject of the present paper. The kinetic model built upon the photophysics characterization of the Rh−Az molecule is outlined in subsection II and the working of the full adder discussed in subsection III. A summary is provided in the Conclusions.

Experimental Methods

Figure 1 shows the newly synthesized[6] bichromophoric molecule used in this study. Commercially available (Aldrich) spectral-grade RhodamineB isothiocyanate, Rh6G (Sigma), and spectral-grade methanol (Riedel-de-Haen) were used without further purification. Standard absorption measurements were made on a Shimadzu UV-1601 UV−vis spectrophotometer, and fluorescence and excitation spectra were taken on a Perkin−Elmer LS 50 spectrofluorimeter, using standard 1 cm length cuvettes.

For most measurements of **Rh**−**Az** emission spectroscopy, a 2.86×10^{-6} M methanol solution, a concentration corresponding approximately to OD = 0.2 for the Rh moiety, at the 545 nm peak of the $S_0 \rightarrow S_1$ absorption, was kept. Highly concentrated solutions of 4×10^{-4} M were used for the characterization of the very weak absorption to the S_1 excited state of the Az moiety at 650 nm in **Rh**−**Az**. No aggregation effects were observed even in these high concentrations.

Laser-induced fluorescence (LIF) experiments were conducted using laser excitation at 532 nm. The laser system (Continuum) operating at a 10 Hz repletion rate used for the LIF experiments was based on a Nd:YAG laser (Powerlite), which produces a Gaussian laser beam shape, with a 0.1 cm^2 cross section, of the fundamental frequency at 1064.1 nm. The fundamental frequency was doubled to generate 532 nm. The different harmonics were separated using a set of dichroic mirrors. The pulse width of the fundamental was 6 ns, and that of the second harmonic was 4 ns. LIF spectra were recorded using a Spectra Pro 275, 0.275 m triple grating monochromator equipped with a stepper motor and a Hammamatsu R-298 photomultipler. The normalized fluorescence signal was processed using a Tektronix TDS 220 two-channel digital oscilloscope, utilizing National Instruments LabView 5.0 software. The photoquenching experiments involved measuring the intensity-dependent LIF. Laser intensities were determined by using an OPHIR model NOVA II power meter.

Results and Discussion

I. Spectroscopic Characterization of the Rhodamine−Azulene Molecular System. We have previously conducted a full spectroscopic and EET investigation of **Rh**−**Az** and of the RhB isocyanate and Az amine chromophores.[7] Absorption spectra of **Rh**−**Az** show that the $S_0 \rightarrow S_1$ absorption band of the Rh moiety is centered at 545 nm, and the $S_0 \rightarrow S_2$ absorption band of the Az one is at 350 nm, with some small contribution from overlap with the $S_0 \rightarrow S_2$ absorption band of the Rh moiety. The $S_0 \rightarrow S_1$ weak absorption of the Az moiety is centered at 645 nm, as a shoulder on the long tail of the Rh moiety $S_0 \rightarrow S_1$ absorption. The assignments are based on the comparison to the corresponding spectra of the separate choromophores.[6,7] These spectra indicate that **Rh**−**Az** is a bichromophoric molecule whose absorption spectrum is a superposition of the absorption spectra of its two chromophores RhB isocyanate and Az amine.[6,7]

The fluorescence spectrum of **Rh**−**Az**, excited at the $S_0 \rightarrow S_1$ transition of its Rh chromophore, showed that the $S_1 \rightarrow S_0$ fluorescence band of the Rh moiety of **Rh**−**Az** is at 572 nm and that the $S_1 \rightarrow S_0$ fluorescence band of the Az moiety, excited by an intramolecular EET process, is at 780 nm.[6,7] In addition, the excitation spectrum of **Rh**−**Az**, monitored at 780 nm, Figure 6, conforms to its absorption spectrum. The differences in the relative intensities of the observed bands between these spectra were analyzed in terms of the quantum yield of the intramolecular EET process in this molecule.[7] The $S_1 \rightarrow S_0$ and $S_2 \rightarrow S_0$ relative fluorescence intensities of **Rh**−**Az** (for both chromophores) were measured.[6,7]

The photophysical characteristics of the **Rh**−**Az** full adder were elucidated by conducting laser photoquenching experiments in which the dependences of the relative fluorescence quantum yield as well as S_2 relative fluorescence intensity on the laser intensity were measured.[8,9] All of these spectroscopic and EET data are summarized in Table 2.

II. Kinetic Modeling of the Photophysics of the Rh−Az Molecule. The rates of the different photophysical processes discussed in subsection I can be represented by the equations

TABLE 2: Spectroscopic Data and PQ and EET Parameters for the Rh−Az Molecular Full Adder

	Rh−Az	
parameter	Rh moiety	Az moiety
τ_{10} (s)	1.2×10^{-9}[b]	1.42×10^{-12}[a]
σ_{01}, cm^2/molec at 18797 cm^{-1}	4.0×10^{-16}[c]	1.2×10^{-18}[c]
Φ_{S_1}	0.95	2×10^{-3}
σ_{12}, cm^2/molec at 18797 cm^{-1}	$(2.2 \pm 0.3)\times10^{-16}$[d]	$(4.5 \pm 0.6)\times10^{-15}$[d]
τ_{12} (s)	0.03×10^{-12}[d]	11.4×10^{-9}[b]
Φ_{S_2}	2×10^{-6}[b]	0.24[b]
$\omega_{S1\rightarrow S0}$, cm^{-1}[e]	17540	13070
$\omega_{S2\rightarrow S0}$, cm^{-1}[e]	27930	27860
k_{ET} (s^{-1})	7.8×10^{9}[c]	

[a] This is the τ_{10} value for **Az**. [b] Data taken from refs 10−13. [c] Refs 8 and 9. [d] Ref 13. [e] Band peak value.[12]

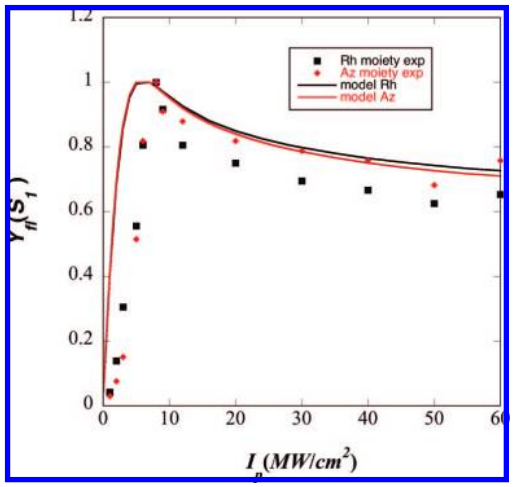

Figure 3. LIF intensities for the $S_1 \rightarrow S_0$ transitions of the Rh (black square) and Az (red diamonds) moieties, normalized to maximum yields, as a function of the intensity of the excitation laser (532 nm). The excitation occurs mainly at the Rh moiety, and there is a fast energy-transfer process to the Az moiety (see parameters in Table 1). The LIF is monitored at 750 nm for Az and at 580 nm for Rh. The full line curves are the result of the kinetic model. The photoquenching of the $S_1 \rightarrow S_0$ emission by absorption to the S_2 state takes place for excitation intensities larger than 7.5 MW/cm^2.[9] Due to the high efficiency of the energy transfer, the absolute value of the LIF yield for the S_1 state of the Rh moiety is 3 orders of magnitude lower than that for the S_1 state of the Az moiety.

of chemical kinetics.[14−17] This is how the kinetic parameters shown in Table 2 were determined. To mimic the temporal evolution of the ensemble of optically excited molecules, we collected together the relevant photophysical processes into a kinetic model. This procedure is well documented in the literature of laser chemistry, for example,[15,17] and has been used already in our earlier letter on this topic.[2] The same procedure has also been used to characterize an intramolecular charge transfer as a route to computation of a full adder.[3]

The processes taken into account in the kinetic modeling are summarized in Figure 2. In addition to the absorption cross sections and the fluorescence lifetimes of the S_1 states of the Rh and Az moieties, the simulations also take the radiative and nonradiative decay processes into account. As shown in ref 7, the intramolecular coupling is weak enough for the S_1 and S_2 states of the Rh and Az moieties to retain their identity. The S_1 states of the Rh and Az moieties decay both radiatively and nonradiatively to the ground state, S_0, of **Rh−Az** molecule, while the S_2 states decay nonradiatively to the S_1 state of their respective moieties and radiatively to the ground state. The radiative and nonradiative rate constants are determined from the fluorescence lifetimes and quantum yield values of the excited states S_1 and S_2 of each moiety. The radiative rate constants are used below to compute the fluorescence yields and compare them with the experimental results.

The excitation laser pulse envelope, $p(t)$, is taken to be Gaussian

$$p(t) = \exp[-(t - t_0)^2/2w^2] \tag{2}$$

with a width, w, of 4 ns for the second harmonic (532 nm), in agreement with the experimental setup discussed in the Experimental Section above.

The flux of the laser pulse is

$$\Phi(t) = \frac{I}{h\nu} p^2(t) \tag{3}$$

The value of the flux at peak height is $\Phi_0 = I/h\nu$; I is the laser intensity and $h\nu = hc/\lambda$, where λ is the laser excitation wavelength.

In reference to Figure 2, the simulation of the time evolution of the populations is obtained from the following set of kinetic equations

$$\begin{aligned}
\frac{dS_0(t)}{dt} &= -(x+y+z)\sigma_{01}^{Rh}\Phi(t)S_0(t) + \left(k_{01nonrad}^{Rn} + k_{01rad}^{Rh}\right)S_1^{Rh}(t) \\
&\quad + k_{02rad}^{Rh}S_2^{Rh}(t) - (x+y+z)\sigma_{01}^{Az}\Phi(t)S_0(t) + \\
&\quad \left(k_{01nonrad}^{Az} + k_{01rad}^{Az}\right)S_1^{Az}(t) + k_{02rad}^{Az}S_2^{Az}(t) \\
\frac{dS_1^{Rh}(t)}{dt} &= +(x+y+z)\sigma_{01}^{Rh}\Phi(t)S_0(t) - \\
&\quad (x+y+z)\sigma_{12}^{Rh}\Phi(t)S_1^{Rh}(t) - \left(k_{01}^{Rh}\right)S_1^{Rh}[t] + k_{12nonrad}^{Rh}S_2^{Rh}(t) - \\
&\quad k_{ET}S_1^{Rh}(t) \\
\frac{dS_2^{Rh}(t)}{dt} &= +(x+y+z)\sigma_{12}^{Rh}\Phi(t)S_1^{Rh}(t) - \\
&\quad (k_{02rad} + k_{12nonrad})S_2^{Rh}(t) \\
\frac{dS_1^{Az}(t)}{dt} &= +(x+y+z)\sigma_{01}^{Az}\Phi(t)S_0(t) - \\
&\quad (x+y+z)\sigma_{12}^{Az}\Phi(t)S_1^{Az}(t) - \left(k_{01}^{Az}\right)S_1^{Az}(t) + k_{12nonrad}^{Az}S_2^{Az}(t) + \\
&\quad k_{ET}S_1^{Rh}(t) \\
\frac{dS_2^{Az}(t)}{dt} &= +(x+y+z)\sigma_{12}^{Az}\Phi(t)S_1^{Az}(t) - \\
&\quad (k_{02rad} + k_{12nonrad})S_2^{Az}(t)
\end{aligned} \tag{4}$$

where x, y, and z represent the binary values of the two inputs of the full adder (x and y) and that of the carry in (z) and $k_{10} = k_{10rad} + k_{10nonrad} = 1/\tau_{10}$. We discuss in the next section the operation of the full adder.

III. Operation of the Full Adder. A full adder has three inputs, the two binary digits to be added, x and y, and the carry in digit (z) coming from the previous addition. Since each is a Boolean variable, there are eight distinct input combinations, as listed in Table 3. This table serves as the truth table for the full addition, listing the values of the two outputs, sum out, and carry out for each input combination. There are only four possible distinct outputs, so that, like many other gates, the

TABLE 3: Encoding of the Inputs and the of the Outputs of the Full Adder

(x, y, z)	I_p	sum out $\equiv Y_{fl}(S_1^{Az})$	carry out $\equiv Y_{fl}(S_2^{Az})$
(0,0,0)	0	0	0
(1,0,0)	$1 \times I_{p0}$	1	0
(0,1,0)	$1 \times I_{p0}$	1	0
(0,0,1)	$1 \times I_{p0}$	1	0
(1,1,0)	$2 \times I_{p0}$	0	1
(1,0,1)	$2 \times I_{p0}$	0	1
(0,1,1)	$2 \times I_{p0}$	0	1
(1,1,1)	$3 \times I_{p0}$	1	1

operation of a full addition is not reversible; given an output, it is not possible to reconstruct a unique input. In the implementation proposed here, the three inputs are provided simultaneously to the bichromophoric **Rh−Az** molecule. The triplets of values of the inputs are encoded into increasing intensities of the excitation laser, whose wavelength is fixed at 532 nm (see Table 3); in other words, a degenerate scheme where $\omega_1 = \omega_2 = \omega_3$ (Table 1) is studied . If only one input has the value 1 (which corresponds to the triplets of inputs (1,0,0), (0,1,0), and (0,0,1)), we define a threshold input intensity, Y_{p0}; when two inputs are 1 (1,1,0), (1,0,1), and (0,1,1), the intensity is $2Y_{p0}$, and when three inputs are 1 (1,1,1), the excitation laser intensity is $3Y_{p0}$. The sum out output is encoded in the LIF of the S_1 state of Az and the carry out in the LIF of the S_2 of Az. The triplet of inputs (1,0,0), (0,1,0), and (0,0,1) must lead to a logical value 1 for the sum out and a logical value 0 for the carry out. On the other hand, the triplets (1,1,0), (1,0,1), and (0,1,1) lead to a sum out of 0 and a carry out of 1, while the triplet (1,1,1) leads to a sum out of 1 and a carry out of 1. The 0 input (0,0,0) corresponds to no excitation so that the two outputs are 0.

The laser operating at 532 nm, used for encoding the inputs, can excite each of the transitions shown in Figure 2. Therefore, in the set of equations in eq 4, it is the sum of the three inputs, $(x + y + z)$ that multiplies the cross sections for each of the four possible absorptions

$$S_0 \xrightarrow{\sigma_{01}^{Rh}} S_1^{Rh} \qquad S_1^{Rh} \xrightarrow{\sigma_{12}^{Rh}} S_2^{Rh} \qquad S_0 \xrightarrow{\sigma_{01}^{Az}} S_1^{Az} \qquad S_1^{Az} \xrightarrow{\sigma_{12}^{Az}} S_2^{Az} \tag{5}$$

The equations in eq 4 were numerically integrated in order to follow populations of the excited states and to compute the different outputs measured experimentally.

The fluorescence yield from the S_1 excited state of the Az moiety is defined as

$$Y_{S_1^{Az}} = k_{10rad}^{Az} \int S_1^{Az}[t]\, dt \tag{6}$$

and that of the Rh moiety is defined accordingly.

The experimental normalized LIF yields, $Y_{S_1}^{Az}$ and $Y_{S_1}^{Rh}$, of the S_1 states of the Az (red diamond) and Rh (black squares) moieties are shown in Figure 3 as a function of the excitation laser intensity, I_p. Also shown in full lines are the results of the kinetic model, computed using eq 6 for a 4 ns pulse envelope (eq 2) by integrating numerically the set of kinetic equations (eq 4). Due to the fast energy-transfer rate between the two moieties, the generic behavior of the LIF yields versus the excitation laser intensity is identical for both; it goes through a maximum at about 8 MW/cm^2 and then decays to a constant value. The maximum at intermediate excitation intensities followed by a plateau at high intensities are indicative of the EET process and of the photoquenching of the $S_1 \rightarrow S_0$ fluorescence by consecutive $S_1 \rightarrow S_2$ excitation.[8,9] The fit between the experimental data and the kinetic model is reasonable; the deviations are mainly due to the large experimental errors and uncertainties in the photophysical parameters of the azulene moiety that were taken from the literature.[10,12,13]

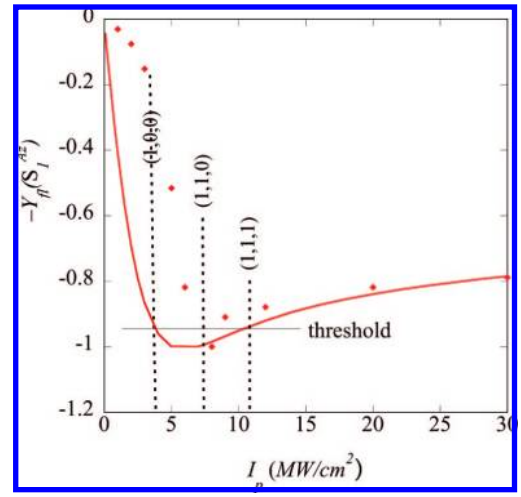

Figure 4. Measured (red diamond) and computed $-Y_{S_1}^{Az}$, normalized to the minimum inverted signal using eqs 4 and 6 (full line) as a function of the excitation laser intensity. One can see that an intensity of 3.5 MW/cm^2 when only one input is 1 allows one to implement the full addition. The threshold for the sum out output is −0.95. For a $-Y_{fl}(S_1)$ of the Az moiety above −0.95, the sum out has the logical value of 1, while below −0.95, it has the logic value 0.

The nonmonotonic behavior of the LIF yield of the S_1 state of the Az moiety allows for the encoding of the sum out. However, the encoding of the sum out requires that the signal goes through a minimum as the excitation laser intensity increases. As can be seen from Table 3, the sum out should be 1 when one of the inputs is 1 (lines 2,3,4), should be 0 when two of the inputs are 1 (lines 5, 6, 7), and should be 0 again when all inputs have the logic value 1 (line 8). Therefore, as a function of the intensity of the laser, for encoding the sum out, one needs a function that goes through a minimum and not through a maximum, as does the fluorescence yield of the S_1 state of Az shown in Figure 3. Therefore, the sum out is defined not as $Y_{S_1}^{Az}$ but as $-Y_{S_1}^{Az}$. $-Y_{S_1}^{Az}$ goes through a minimum at ≈7.5 MW/cm^2 (see Figure 4) and can be directly obtained experimentally by recording the inverted fluorescence signal.

In addition, Figures 3 and 4 allow for the determination of the value of the increment in the laser intensity, I_{p0}, used to encode the inputs and the threshold value of intensity used to determine the logical value of the sum out output. As shown in Table 3, if only one input has the logic value of 1, which corresponds to lines 2 (1,0,0), 3 (0,1,0) and 4 (0,0,1) of Table 3), the intensity is I_{p0}, if two inputs are equal to 1 (line 5 (1,1,0), line 6 (1,0,1), and line 7 (0,1,1) of Table 3), the intensity is $2I_{p0}$, while when the three inputs are 1 (line 8 (1,1,1) of Table 2), the input intensity is $3I_{p0}$. For all inputs equal to 0 (0,0,0), the input laser is off. From Figures 3 and 4, we define I_{p0} to be 3−4 MW/cm^2. For the sum out output, a value of the normalized LIF yield from the S_1 state of the Az moiety below −0.95 corresponds to a logic value of 0, while above −0.95, the sum out is 1.

Figures 5 and 6 are the analogue of Figure 3, but for the normalized experimental and fitted LIF yield from the S_2 states of the Rh and the Az moieties. One can see that while both moieties exhibit the same generic curve, their dependence with

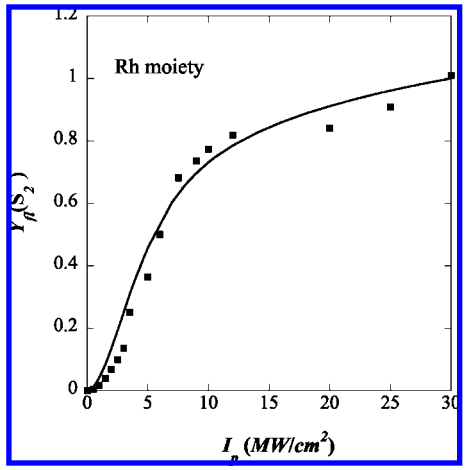

Figure 5. Normalized LIF yield of the S_2 of the Rh moiety as a function of the excitation laser intensity at 532 nm, monitored at 330 nm. At low intensities, the dependence of $Y_{fl}(S_2)$ is quadratic due to two-photon consecutive absorption. The full line is the fit to the kinetic model.

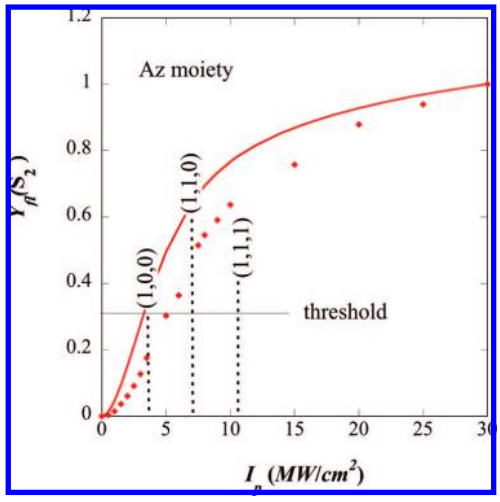

Figure 6. Normalized LIF yield of the S_2 of the Az moiety as a function of the excitation laser intensity at 532 nm. At low intensities, the dependence of $Y_{fl}(S_2)$ is quadratic due to two-photon consecutive absorption. The full line is the fit to the kinetic model. Also shown are the three intensities used to encode the inputs as well as the threshold value of $Y_{fl}(S_2)$ that is used to distinguish between a carry out value of 0 and a carry out value of 1. See the text for more details.

respect to the intensity of the excitation laser is different from that of the S_1 states. This is what allows us to use the LIF yield from the S_2 state of the Az moiety for encoding the carry out, as explained below. The LIF of the S_2 state of the Az moiety is computed using

$$Y_{S_2^{Az}} = k_{20rad}^{Az} \int S_2^{Az}[t]\, dt \qquad (7)$$

and that of the S_2 of the Rh moiety is computed accordingly.

Both curves in Figures 5 and 6 show a quadratic increase of $Y_{fl}(S_2)$ at low intensity due to consecutive two-photon absorption and then saturate to their maximal value at high intensity. In terms of their absolute values, the LIF intensity from the Az moiety is four orders of magnitude larger than that of the Rh moiety. The reason is that because of the fast intramolecular rate from the Rh moiety to the Az moiety, at intermediate intensities, the excitation from the S_1 state of Az to the S_2 of Az is more probable than that from the S_1 state of Rh to the S_2 state of Rh. Another point to note is that because of the unusually low absorption cross section of the S_1 state of Az, even at high intensities, the main absorption is to the S_1 state of the Rh moiety, which is transferred very efficiently to the S_1 state of Az by intramolecular energy transfer. For this reason, we propose to detect the carry out by monitoring the fluorescence from the S_2 of the Az moiety only.

As can be seen from Table 2, the carry out is 0 when one input is 1 ((1,0,0), (0,1,0), and (0,0,1)) and 1 whether two or three inputs are equal to 1. Figure 6 allows us to determine the threshold intensity for the carry out logical output. If the LIF S_2 yield falls in the range of [0,0.2], the logical value of the carry out is 0, while if it is above 0.4, the carry out is 1.

Conclusions

We have shown how an all-optical full adder logic circuit can be implemented in the newly synthesized azulene−amine bichromophoric molecule by utilizing combinations of one- and two-photon absorptions for the input signals and LIF fluorescence intensity from the S_1 and S_2 states of the Az moiety as sum out and carry out logic outputs. The excitation at 532 nm used for encoding the inputs can take place at both sites, but because of the unusually low cross section for the $S_0 \rightarrow S_1$ transition of Az moiety, it predominantly occurs at the Rh moiety. The photon absorbed is then efficiently transferred to the S_1 state of the Az moiety by EET, where a second photon can induce the $S_1 \rightarrow S_2$ transition. The latter is favored over the $S_1 \rightarrow S_2$ transition at the Rh moiety by a higher cross section (one order of magnitude larger).

The two outputs of the full adder are obtained directly by monitoring the LIF intensity of the S_1 state (sum out) and that of the S_2 state (carry out) of the Az moiety and can be measured independently. The working of the full adder scheme therefore relies on the intramolecular transfer of information from the S_1 state of the Rh moiety to the S_1 of the Az. However, this scheme does not correspond to the implementation of a full addition by concatenation of two half adders. As such, the logic scheme proposed here shows that the photophysical characteristics of molecules can provide for molecular logic implementations that are different from those devised for switching circuits.

Acknowledgment. The work of F.R. and R.D.L. is supported by the EC FET-open STREP Project MOLDYNLOGIC and the NoE FAME. The technical help of Naser Shakkour is highly appreciated.

References and Notes

(1) Mano, M. M.; Kime, C. R. *Logic and Computer Design Fundamentals*; Prentice Hall: Upper Saddle River, NJ, 2000.
(2) Remacle, F.; Speiser, S.; Levine, R. D. *J. Phys. Chem. A* **2001**, *105*, 5589–5591.
(3) Remacle, F.; Weinkauf, R.; Levine, R. D. *J. Phys. Chem. A* **2006**, *110*, 177–184.
(4) Speiser, S.; Van der Werf, R.; Kommandeur, J. *Chem. Phys.* **1973**, *1*, 297–305.
(5) Speiser, S.; Shakkour, N. *App. Phys. B* **1985**, *38*, 191–197.
(6) Salman, H.; Eichen, Y.; Speiser, S. *Mater. Sci. Eng., C* **2006**, *26*, 881–885.
(7) Kuznetz, O.; Davis, D.; Salman, H.; Eichen, Y.; Speiser, S. *J. Photochem. Photobiol., A* **2007**, *191*, 176–181.
(8) Kuznetz, O.; Salman, H.; Shakkour, N.; Eichen, Y.; Speiser, S. *Chem. Phys. Lett.* **2008**, *451*, 63–67.
(9) Kuznetz, O.; Salman, H.; Shakkour, N.; Eichen, Y.; Speiser, S. *Mol. Phys.* **2008**, *106*, 531–535.
(10) Wagner, B. D.; Szymanski, M.; Steer, R. P. *J. Chem. Phys.* **1993**, *98*, 301–307.
(11) Speiser, S. *Appl. Phys. B* **1989**, *49*, 109–112.
(12) Kaplan, I.; Jortner, J. *Chem. Phys.* **1978**, *32*, 381–396.

(13) Orner, G. C.; Topp, M. R. *Chem. Phys. Lett.* **1975**, *36*, 295−300.

(14) Bernstein, R. B. *Chemical Dynamics via Molecular Beam and Laser Techniques*; Oxford University Press: New York, 1982.

(15) VanHecke, G. R.; Karukstis, K. K. *A Guide to Lasers in Chemistry*; Jones and Bartlett: Boston, MA, 1998.

(16) Levine, R. D. *Molecular Reaction Dynamics*; Cambridge University Press: Cambridge, U.K., 2005.

(17) Shaul, A. B.; Haas, Y.; Kompa, K. L.; Levine, R. D. *Lasers and Chemical Change*; Springer: Berlin, Germany, 1982.

JP804658B